A Compendium of Directional Calculations Based on the Minimum Curvature Method

S.J. Sawaryn, SPE, and **J.L. Thorogood,** SPE, BP plc

Summary

The minimum curvature method has emerged as the accepted industry standard for the calculation of 3D directional surveys. Using this model, the well's trajectory is represented by a series of circular arcs and straight lines. Collections of other points, lines, and planes can be used to represent features such as adjacent wells, lease lines, geological targets, and faults. The relationships between these objects have simple geometrical interpretations, making them amenable to mathematical treatment. The calculations are now used extensively in 3D imaging and directional collision scans, making them critical for both business and safety. However, references for the calculations are incomplete, scattered in the literature, and have no systematic mathematical treatment. These features make programming a consistent and reliable set of algorithms more difficult. Increased standardization is needed.

Investigation shows that iterative schemes have been used in situations in which explicit solutions are possible. Explicit calculations are preferred because they confer numerical predictability and stability. Though vector methods were frequently adopted in the early stages of the published derivations, opportunities for simplification were missed because of premature translation to Cartesian coordinates.

This paper contains a compendium of algorithms based on the minimum curvature method (includes coordinate reference frames, toolface, interpolation, intersection with a target plane, minimum and maximum true vertical depth (TVD) in a horizontal section, point closest to a circular arc, survey station to a target position with and without the direction defined, nudges, and steering runs). Consistent vector methods have been used throughout with improvements in mathematical efficiency, stability, and predictability of behavior. The resulting algorithms are also simpler and more cost effective to code and test. This paper describes the practical context in which each of the algorithms is applied and enumerates some key tests that need to be performed.

Introduction

The first reference to the minimum curvature method is credited to Mason and Taylor[1] in 1971. In the same year, Zaremba[2] submitted an identical algorithm that he termed "the circular arc" method. In the minimum curvature method, two adjacent survey points are assumed to lie on a circular arc. The arc is located in a plane, the orientation of which is defined by the known inclination and direction angles at the ends. By 1985, the minimum curvature method was recognized by the industry as one of the most accurate methods, but was regarded as cumbersome for hand calculation.[3,4] The emergence of well-trajectory planning packages to help manage directional work in dense well clusters increased its popularity. It was natural to use the same model for both the surveys and the segments of the well-plan trajectories. Today, with the widespread use of computers, computational power is no longer an issue, and the method has emerged as the accepted industry standard.

This paper (SPE 84246) was first presented at the 2003 SPE Annual Technical Conference and Exhibition, Denver, 5–8 October, and revised for publication. Original manuscript received for review 27 January 2004. Revised manuscript received 15 January 2005. Paper peer approved 29 January 2005.

Industry Requirements

Over the years, various algorithms based on the minimum curvature method have been published for the construction of increasingly complex trajectories and tasks, such as interpolation. Because these algorithms have emerged piecemeal, they have tended to use different nomenclatures and mathematical techniques for their solution. The result of this piecemeal development is duplicated and inefficient computer code and a poor understanding of the engineering integrity of the systems.

Safety and Business Criticality. An undetected fault in the coding or use of directional-surveying and collision-scanning software has been classified as having the potential to cause property damage, environmental damage, personal injury, or loss of reputation.[5] The integrity of these business- and safety-critical drilling systems is, therefore, a concern. Modern 3D imaging and directional-scanning packages execute thousands of calculations for each task. Increased automation of the workflows associated with these tasks means that most calculations must be taken for granted and will pass unchecked. Sawaryn *et al.*[6] have described a process for managing these systems, and identified a number of requirements related to the equations they use. Specifically, equations must be traceable back to the source documentation, which must clearly explain their purpose, limitations, and use. The general characteristics of the published algorithms can be assessed against these requirements.

Angular Change. Like other survey calculation methods, the minimum curvature algorithm was originally developed to calculate a well's position from directional surveys. The spacing between the survey stations was normally 30 to 500 ft. At that time, with typical build rates, the total-angle change over a 100-ft course length would rarely be allowed to exceed 5° and the final inclination of most of these early wells was below 90°. When creating directional well plans, the total-angle change between adjacent stations in the plan may be considerably larger. These days, in designer wells, the angular change between two adjacent points on a well plan may exceed 90°, and the final inclination often exceeds 90°. One well[7] is recorded as having reached 164.7° inclination. Many of the published algorithms do not contain an explicit definition of the maximum permitted angle change. The multiple solutions arising from periodicity of the trigonometric equations involved makes this a serious concern.

Mathematical Behavior. The possibility of multiple solutions means the results of the calculations may not always be as intended, unless great care has been paid to their implementation. Some algorithms employ iterative schemes so that even if the scheme converges, there is no guarantee that it converges to the correct solution. Ideally, iterative schemes should be accompanied by proof of convergence. At the very least, they should be thoroughly tested over some specified range of variables. Additionally, there are cases for which no solution exists and extra code is needed to trap this condition. Explicit expressions are more predictable and usually confer advantages in speed and maintainability of the computer code.

For certain values (for example, in geometrically straight hole), expressions may be indeterminate. One solution, adopted by Zaremba,[2] is to define a suitably small number at which the expression jumps abruptly to the asymptotic value. However, this can give rise to random differences between software packages.[6] A

better method is to develop series expressions that enable a smooth transition to be maintained.

Common Constructs. The absence of consistent mathematical methods and nomenclature may hide common constructs and potential simplifications in the coding of the algorithms. For example, an equation in the form $C = A\sin(\alpha) + B\cos(\alpha)$ appears in many of the geometric constructions associated with the minimum curvature method. This equation can be solved explicitly for α, and several mathematically equivalent forms exist. Zaremba[2] proposed the form (see Eq. 1) that is used throughout this paper:

$$\alpha = 2\tan^{-1}\left[\frac{A \pm (A^2 + B^2 - C^2)^{\frac{1}{2}}}{B + C}\right]. \quad \ldots\ldots\ldots\ldots\ldots\ldots (1)$$

When presented in this way, it can be seen that no real solutions exist if $C^2 > A^2 + B^2$. This inequality has simple geometric interpretations and several examples of its use are highlighted in this paper.

Inconsistent nomenclature also leads to implemenational difficulties. Review shows the nomenclatures used in the literature are neither consistent with each other, nor consistent with accepted mathematical practice. One example is the definition of the normal vector that mathematical convention has pointing towards the center of curvature. This is opposite to the convention used in the earlier drilling literature. Because of the expansion in directional-drilling applications, symbols inevitably conflict. The Industry Steering Committee on Wellbore Survey Accuracy has proposed some standards,[8] but with limited scope. We assert that the SPE documentation standards[9] associated with this subject area are no longer adequate and need revising.

Directional Calculations

A consistent vector notation is used throughout this paper. This simplifies the development of the 3D equations and improves the clarity and presentation of the results. For convenience, the main vector operations are summarized in the Appendix. In some cases, series expansions have been used to ensure the smooth transition of an expression into what would otherwise be an indeterminate form. The thresholds at which the series approximations should be used depend on the machine precision. The constants used in this paper assume calculations are good to at least nine significant digits. The angle α subtending the arc may assume values such that $0 \le \alpha < \pi$. Throughout, it is also assumed that the start and end points of the arc are not coincident. Until such time as the standards are officially revised, we have chosen to maintain commonality with earlier papers on this subject and use a vector $\underline{b}$ pointing away from the center of the arc. For comparison with mathematical texts, the normal vector is, therefore, $-\underline{b}$.

Reference Frames. ***Coordinate Reference Frame.*** The traditional reference frame for directional work uses north, east, and vertical coordinates that comprise a right-handed set, as shown in **Fig. 1.** A point *N,E,V* can be represented by the vector $\underline{p}$ in Eq. 2.

$$\underline{p} = \begin{bmatrix} N \\ E \\ V \end{bmatrix}. \quad \ldots\ldots\ldots\ldots\ldots\ldots\ldots\ldots\ldots\ldots\ldots\ldots (2)$$

A unit direction vector $\underline{t}$ can be represented in terms of the local inclination θ and azimuth ϕ, as shown in Eq. 3. The inclination and azimuth values can be calculated from the vector's components using the expressions in Eqs. 4 and 5.

$$\underline{t} = \begin{bmatrix} \Delta N \\ \Delta E \\ \Delta V \end{bmatrix} = \begin{bmatrix} \sin\theta\cos\phi \\ \sin\theta\sin\phi \\ \cos\theta \end{bmatrix}. \quad \ldots\ldots\ldots\ldots\ldots\ldots (3)$$

$$\theta = \tan^{-1}\left[\frac{(\Delta N^2 + \Delta E^2)^{\frac{1}{2}}}{\Delta V}\right]. \quad \ldots\ldots\ldots\ldots\ldots\ldots\ldots (4)$$

$$\phi = \tan^{-1}\left(\frac{\Delta E}{\Delta N}\right). \quad \ldots\ldots\ldots\ldots\ldots\ldots\ldots\ldots\ldots (5)$$

By using this reference frame, an implicit assumption is made that the Earth is flat. For moderate distances from the origin, this assumption holds. For larger distances, such as those encountered in extended-reach wells, the Earth's curvature is important and corrections to the coordinates must be made. Williamson and Wilson[10] discuss the matter in detail.

Borehole Reference Frames. Two reference frames are associated with the borehole, see **Fig. 2.** The first frame is formed by the highside, rightside, and tangent unit vectors $\underline{h}$, $\underline{r}$, and $\underline{t}$, respectively. These form a right-handed, mutually orthogonal set. In curved hole, the second frame comprises the normal, binormal, and tangent unit vectors $-\underline{b}$, $\underline{n}$, and $\underline{t}$, respectively. These also form a right-handed, mutually orthogonal set. The angle between the highside vector $\underline{h}$ and normal vector $-\underline{b}$ is the toolface angle, τ.

The highside, rightside, and vertical unit vectors are represented in Eqs. 6, 7, and 8. Expressions for the normal and binormal vectors $-\underline{b}$ and $\underline{n}$ can be found in the Appendix (Eqs. A-8 through A-12).

$$\underline{h} = \begin{bmatrix} \cos\theta\cos\phi \\ \cos\theta\sin\phi \\ -\sin\theta \end{bmatrix}, \quad \ldots\ldots\ldots\ldots\ldots\ldots\ldots\ldots (6)$$

$$\underline{r} = \begin{bmatrix} -\sin\phi \\ \cos\phi \\ 0 \end{bmatrix}, \quad \ldots\ldots\ldots\ldots\ldots\ldots\ldots\ldots\ldots (7)$$

$$\underline{v} = \begin{bmatrix} 0 \\ 0 \\ 1 \end{bmatrix}. \quad \ldots\ldots\ldots\ldots\ldots\ldots\ldots\ldots\ldots\ldots (8)$$

Dogleg Severity. Dogleg severity is a measure of the change in inclination and/or direction of a borehole, see **Fig. 3.** The change

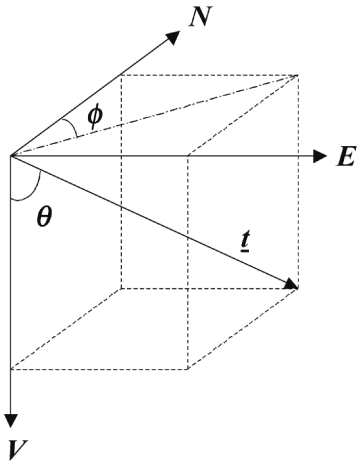

Fig. 1—North, east, and vertical coordinate reference frame.

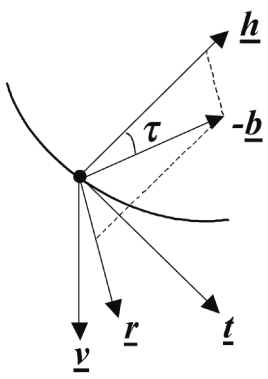

Fig. 2—Borehole reference frames, including the toolface angle τ.

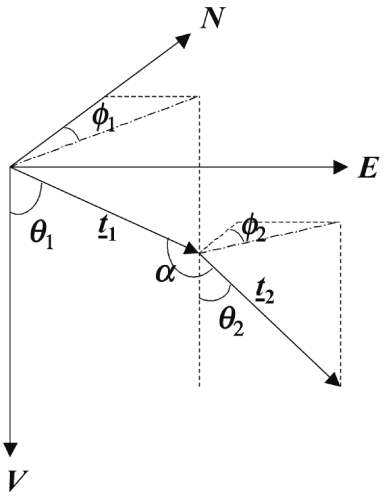

Fig. 3—A dogleg defined by the two direction vectors $\underline{t}_1$ and $\underline{t}_2$.

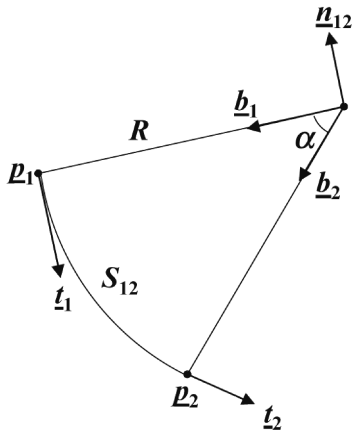

Fig. 4—The geometry of the minimum curvature between two adjacent survey points.

is usually expressed in degrees per 100 ft of course length in oilfield units[3] and degrees per 30 m in metric units. Dogleg severity is used to determine stress fatigue in drillpipe, casing wear, and casing design loads. It can also be a limiting factor in casing running and directional-drilling operations. For the minimum curvature method, the expression for the dogleg severity takes the form of $(18{,}000^*\alpha/\pi)/(D_2-D_1)$ in oilfield units. The difference in measured depths, D_2-D_1, between the points is referred to as the course length, S_{12}.

Most expressions found in the literature involve the calculation of an arc cosine. These have been used even though it is recognized that cosines of small angles are more difficult to handle than sines of small angles. Eq. 9, developed by Lubinski,[3] does not make any assumption about the actual path of the wellbore, yet it is mathematically equivalent to the expression traditionally used in the minimum curvature method. An expression for $\tan(\alpha/2)$ is readily developed from it:

$$\alpha = 2\sin^{-1}\left\{\left[\sin^2\left(\frac{\theta_2-\theta_1}{2}\right)+\sin\theta_1\sin\theta_2\sin^2\left(\frac{\phi_2-\phi_1}{2}\right)\right]^{\frac{1}{2}}\right\}. \quad \ldots\ldots\ldots\ldots (9)$$

Because the trigonometrical identity and computational advantages of Eq. 9 were recognized, it is surprising that it has not been adopted sooner. The dogleg severity can be related to both the radius of curvature and the curvature, κ, of the arc, by use of the relationships (see Eq. 10):

$$\kappa = \frac{1}{R} = \frac{\alpha}{S_{12}} = \frac{\alpha^*}{S^*}. \quad \ldots\ldots\ldots\ldots (10)$$

Survey Calculation. Accurate determination of wellbore position is critical to well placement, collision avoidance, reservoir modeling, and equity determination. Though the accuracy of the minimum curvature method is acknowledged, Stockhausen and Lesso[11] showed that modern drilling practices could introduce systematic errors, even with survey intervals as frequent as 100 ft.

The position of the next survey point, $\underline{p}_2$, is calculated from $\underline{p}_1$ by use of Eq. 11, see **Fig. 4.** The shape factor $f(\alpha)$ equals $\tan(\alpha/2)/(\alpha/2)$. Details are summarized in the Appendix (Eqs. A-6 through A-17).

$$\underline{p}_2 = \underline{p}_1 + \frac{S_{12}f(\alpha)}{2}\begin{bmatrix}\sin\theta_1\cos\phi_1+\sin\theta_2\cos\phi_2\\ \sin\theta_1\sin\phi_1+\sin\theta_2\sin\phi_2\\ \cos\theta_1+\cos\theta_2\end{bmatrix}. \quad \ldots\ldots\ldots (11)$$

Straight-Hole Conditions. When α equals 0, the shape factor is mathematically indeterminate, so for $\alpha<0.02$ radians, the series expansion (Eq. 12) should be used instead.[12] The series is presented in Horner[13] form to minimize both the number of arithmetic operations and the propagation of errors:

$$f(\alpha) \approx 1+\frac{\alpha^2}{12}\left\{1+\frac{\alpha^2}{10}\left[1+\frac{\alpha^2}{168}\left(1+\frac{31\alpha^2}{18}\right)\right]\right\}. \quad \ldots\ldots\ldots (12)$$

There is a second possible solution for Eq. 9, which is equal to $(2\pi-\alpha)$. The measured depth between the survey stations must be the same in both cases, implying the second solution has a greater curvature, see **Fig. 5.** When calculating directional surveys, the density of survey stations, behavior of the bottomhole assemblies, and knowledge of the toolface settings means this situation is of no practical concern. This may not be the case for adjacent points in a well-plan trajectory, which may be separated by considerable distances.

Interpolation. This is often required to identify the coordinates of a particular point, for example, $\underline{p}^*$ on a trajectory, see **Fig. 6.** In all cases, the problem reduces to one of interpolation or extrapolation on an arc, defined by the positions $\underline{p}_1$ and $\underline{p}_2$ and directions $\underline{t}_1$ and $\underline{t}_2$ of its end points. The algorithms presented here may be used for both functions. The interpolation may be driven by one of several parameters, such as measured depth, subtended angle, inclination, azimuth, northing, easting, or vertical ordinate.

Before discussing each of these cases, it is worth reviewing the properties of a circular arc. The subtended angle, inclination, and azimuth of a point on a circular arc can be determined solely by the attitude of the circle in the coordinate reference frame. Knowledge of the size of the circle enables course lengths to be determined. Finally, it is only if a north, east, or vertical ordinate is needed that the absolute position of the circle in the reference frame must be defined.

Interpolation on Measured Depth. The association of events or observations, such as formation tops and overpulls with points on the wellbore, is a common requirement. Interpolations on measured depth determined from the pipe tally are, therefore, the most common interpolation mode. If S^* is the course length along the

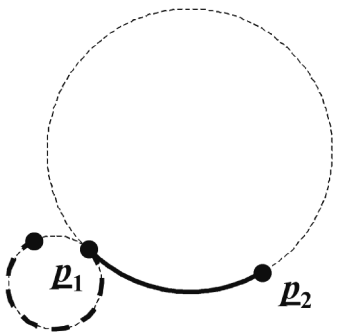

Fig. 5—The two possible mathematical solutions.

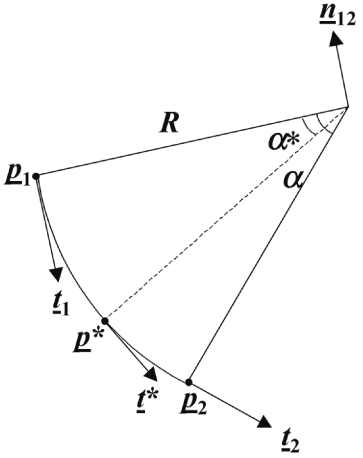

Fig. 6—Interpolation at a point $\underline{p}^*$ on a circular arc.

arc at which the properties are required, the relationships $\alpha^* = (S^*/S_{12})\alpha$ and $(\alpha-\alpha^*) = (1-S^*/S_{12})\alpha$ can be used to reduce the interpolation on measured depth to the interpolation on subtended angle (see Eq. 13).

Interpolation on Subtended Angle. Eq. 13 enables the direction vector, $\underline{t}^*$, at a point $\underline{p}^*$ on an arc to be determined solely from the direction vectors of its start and end points and the angle subtended from the first point $\underline{p}_1$ to the point of interest. Refer to the Appendix (Eqs. A-18 through A-26).

$$\underline{t}^* = \frac{\sin(\alpha-\alpha^*)}{\sin\alpha}\underline{t}_1 + \frac{\sin\alpha^*}{\sin\alpha}\underline{t}_2. \quad \ldots\ldots\ldots\ldots\ldots\ldots\ldots\ldots (13)$$

Many of the algorithms presented in this paper involve the determination of the subtended angle α^* as a first step. The relationship in Eq. 13 provides a convenient means of determining the other parameters at the point, once the subtended angle has been found. For example, once $\underline{t}^*$ is known, the corresponding point $\underline{p}^*$ can be calculated using the minimum curvature equation (Eq. 11).

Straight-Hole Conditions. When the subtended angle, α, equals zero, both terms in Eq. 13 are indeterminate. For $\alpha<0.02$ radians, these terms that contain factors of the form $\sin(c\alpha)/\sin\alpha$ may be expanded[14] in another Horner series (see Eq. 14):

$$\frac{\sin(c\alpha)}{\sin\alpha} \approx c + \alpha^2\left[c\left(\frac{1}{6}-\frac{c^2}{6}\right) + \alpha^2\left\{c\left[\frac{7}{360}+c^2\left(\frac{-1}{36}+\frac{c^2}{120}\right)\right]\right.\right.$$
$$+ \alpha^2\left(c\left\{\frac{31}{15{,}120}+c^2\left[\frac{-7}{2{,}160}+c^2\left(\frac{1}{720}-\frac{c^2}{5{,}040}\right)\right]\right\}\right.$$
$$+ c\alpha^2\left(\frac{127}{604{,}800}+c^2\left\{\frac{-31}{90{,}720}+c^2\left[\frac{7}{43{,}200}\right.\right.\right.$$
$$\left.\left.\left.\left.\left.\left.+ c^2\left(\frac{-1}{30{,}240}+\frac{c^2}{362{,}880}\right)\right]\right\}\right)\right)\right\}\right]. \quad \ldots\ldots\ldots\ldots (14)$$

It should be noted that this interpolation mode is impossible when the subtended angle is identically 0, unless the constant, c, can be defined in some other way, such as by use of the ratio of the course lengths.

Interpolation on Azimuth. Occasionally, it is necessary to truncate a well-plan trajectory at a depth so that it is lined up with a specified direction. First, check the condition $\sin\theta_1 \sin\theta_2 \sin(\phi_2-\phi_1)\neq 0$ to determine that the arc does not lie in the vertical plane and that a solution exists. The subtended angle is then determined by use of Eq. 15:

$$\alpha^* = \tan^{-1}\left[\frac{\sin(\phi_1-\phi^*)\sin\alpha\,\sin\theta_1}{\sin(\phi^*-\phi_2)\sin\theta_2 + \sin(\phi_1-\phi^*)\sin\theta_1\cos\alpha}\right]. \quad \ldots\ldots\ldots\ldots (15)$$

The Appendix shows that Eq. A-28, used to calculate the inclination θ^* from ϕ^* and α^*, is of the form $C = A\sin(\theta^*) + B\cos(\theta^*)$. The solution for θ^* is determined using Eq. 1. In this case, the constants A, B, and C are given by Eqs. 16, 17, and 18, respectively. Choose the smallest root, unless it is less than or equal to both θ_1 and θ_2, in which case, the largest root should be chosen.

$$A = \sin\theta_1\cos(\phi^*-\phi_1), \quad \ldots\ldots\ldots\ldots (16)$$

$$B = \cos\theta_1, \quad \ldots\ldots\ldots\ldots (17)$$

$$C = \cos\alpha^*. \quad \ldots\ldots\ldots\ldots (18)$$

As the subtended angle was originally determined from an azimuth on the arc, a solution must exist. Finally, the position $\underline{p}^*$ is determined using the minimum curvature equation (Eq. 11). Generally, if $C^2 > A^2+B^2$, the orientation of the arc is too shallow for the inclination at any point on it to reach the desired value. For details, see the Appendix (Eqs. A-27 through A-29).

Straight-Hole Conditions. Azimuth varies linearly with measured depth in near-straight-hole conditions. For angle $\alpha<10^{-4}$ radians, Eq. 19 should be used to determine the corresponding measured depth. If the azimuth values in either the numerator or denominator straddle north, the minimum angular difference should be used. The remaining properties can be determined by interpolating on this depth:

$$S^* \approx S_{12}\left(\frac{\phi^*-\phi_1}{\phi_2-\phi_1}\right). \quad \ldots\ldots\ldots\ldots (19)$$

Interpolation on Inclination. The determination of measured depths corresponding to some inclination range appears in the automation of calculations for hole cleaning and rock mechanics. First, check that both points θ_1 and θ_2 are not equal to $\pi/2$. In this condition, the arc would lie in the horizontal plane and no solutions are possible. In the Appendix (Eq. A-30), it is shown that the subtended angle α^* can be calculated with Eq. 1. In this case, the constants A, B, and C are given by Eqs. 20 through 22:

$$A = \cos\theta_2 - \cos\alpha\cos\theta_1 \quad \ldots\ldots\ldots\ldots (20)$$

$$B = \sin\alpha\cos\theta_1 \quad \ldots\ldots\ldots\ldots (21)$$

$$C = \sin\alpha\cos\theta^* \quad \ldots\ldots\ldots\ldots (22)$$

If $C^2 > A^2 + B^2$, then the orientation of the plane containing the arc is too close to the horizontal plane to enable the desired inclination to be reached; no solutions exist. The corresponding azimuth value can be determined from Eq. 23:

$$\phi^* = \tan^{-1}\left[\frac{\sin\theta_1\sin\phi_1\sin(\alpha-\alpha^*) + \sin\theta_2\sin\phi_2\sin\alpha^*}{\sin\theta_1\cos\phi_1\sin(\alpha-\alpha^*) + \sin\theta_2\cos\phi_2\sin\alpha^*}\right]. \quad \ldots\ldots\ldots\ldots (23)$$

Straight-Hole Conditions. Inclination varies linearly with measured depth in near-straight-hole conditions. For the subtended angle, $\alpha < 10^{-4}$ radians, Eq. 24 should be used to determine the course length. The remaining properties can be determined by interpolating on this depth:

$$S^* \approx S_{12}\left(\frac{\theta^*-\theta_1}{\theta_2-\theta_1}\right). \quad \ldots\ldots\ldots\ldots (24)$$

Interpolation at a Plane. A plane can be used to represent many geological features, such as formation horizons and faults. In 3D visualization tools, collections of interlocking planes are used to represent complex geological features. Imaginary planes can be used to represent lease boundaries, or the north, east, and vertical limits, on directional plots. The point $\underline{p}^*$ at which the well meets or crosses these features, is of great practical interest, see **Fig. 7.** The plane is uniquely defined by its normal vector $\underline{m}$ and any point $\underline{p}_x$ on it.

There are five possible relationships between the arc and the plane:

- An infinite number of intersections—when the plane containing the arc and the target plane are parallel. This condition should be tested first by establishing if both $(\underline{m}\cdot\underline{t}_1)$ and $(\underline{m}\cdot\underline{t}_2)$ are equal to 0.
- Two intersections—when the arc completely cuts the plane.

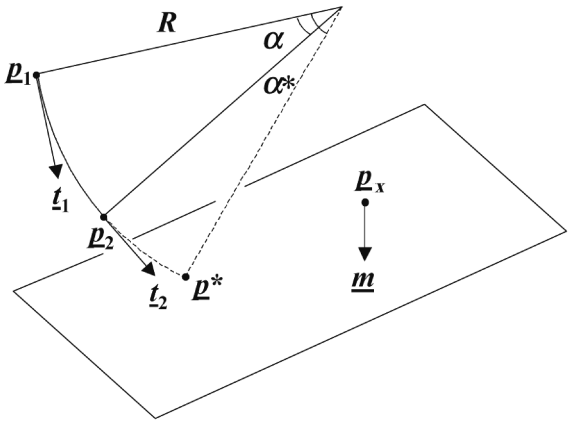

Fig. 7—The intersection (extrapolation) of a circular arc and a plane at a point $\underline{p}^*$.

- One intersection—when the arc just touches the plane.
- No intersections—when the curvature of the arc is too large.
- If curvature is very small, then, for practical purposes, the problem is reduced to the intersection of a straight line with a plane.

The Appendix (Eqs. A-31 to A-35) shows that the subtended angle, α^*, to the plane can be calculated with Eq. 1. In this case, the constants A, B, and C are given by Eqs. 25 through 27:

$$A = (\underline{m} \cdot \underline{t}_1)\sin\alpha, \quad \ldots\ldots\ldots\ldots\ldots\ldots\ldots\ldots\ldots\ldots\ldots\ldots (25)$$

$$B = (\underline{m} \cdot \underline{t}_1)\cos\alpha - (\underline{m} \cdot \underline{t}_2), \quad \ldots\ldots\ldots\ldots\ldots\ldots\ldots\ldots\ldots\ldots (26)$$

$$C = \frac{\underline{m} \cdot (\underline{p}_x - \underline{p}_1)\alpha \sin\alpha}{S_{12}} + (\underline{m} \cdot \underline{t}_1)\cos\alpha - (\underline{m} \cdot \underline{t}_2). \quad \ldots\ldots\ldots\ldots (27)$$

If $C^2 > A^2 + B^2$, the curvature of the arc is too large to intersect the plane and no solutions exist. If $C^2 = A^2 + B^2$, then the arc just touches the plane and there is only one solution. For $C^2 < A^2 + B^2$, there are two intersections and, in this case, the subtended angles to both of them may be less than π. The two solutions correspond to the plus and minus signs in Eq. 1. This situation may be encountered when landing in a pay zone and the assembly is not building at the desired rate. Using this interpolation mode, it is possible to determine if and at what point the bottom of the zone will be breached and the point at which the well is expected to re-enter. The lost-production interval can then be calculated directly.

Straight-Hole Conditions. When the subtended angle α equals 0, the above solution is indeterminate. For $\alpha < 10^{-4}$ radians, a series expansion (see Eq. 29) is used to determine the measured depth; see the Appendix (Eqs. A-36 through A-43). No solution is possible if the line is parallel to the plane when $(\underline{m} \cdot \underline{t}_1)$ equals 0:

$$\zeta = \frac{\underline{m} \cdot (\underline{p}_x - \underline{p}_1)[(\underline{m} \cdot \underline{t}_2) - (\underline{m} \cdot \underline{t}_1)]}{S_{12}(\underline{m} \cdot \underline{t}_1)^2}, \quad \ldots\ldots\ldots\ldots\ldots\ldots (28)$$

$$S^* \approx \frac{\underline{m} \cdot (\underline{p}_x - \underline{p}_1)}{(\underline{m} \cdot \underline{t}_1)}\left[1 - \frac{\zeta}{2}(1 - \zeta)\right]. \quad \ldots\ldots\ldots\ldots\ldots\ldots (29)$$

Orientation of the Target Plane. The normal vector $\underline{m}$, defining the orientation of the target plane, can be constructed in terms of the dip angle, Θ, and dip azimuth, Φ, of the plane according to Eq. 30:

$$\underline{m} = \begin{bmatrix} -\sin\Theta\cos\Phi \\ -\sin\Theta\sin\Phi \\ \cos\Theta \end{bmatrix} \quad \ldots\ldots\ldots\ldots\ldots\ldots\ldots\ldots\ldots\ldots (30)$$

North, East, and Vertical Interpolation. The interpolations on north, east, or vertical ordinates are particular cases of the more general expression. The values of the vectors $\underline{p}_x$ and $\underline{m}$ to use in each of these are listed in **Table 1.** For example, if the well is building and approaching an eastern lease line, use the vectors listed under the heading "East," with E^* set equal to the numeric value of the eastern boundary limit.

TABLE 1—CHOICE OF VECTORS $\underline{p}_x$ AND $\underline{m}$ FOR INTERPOLATING ON NORTH, EAST, AND VERTICAL ORDINATES

	North	East	Vertical
$\underline{p}_x$	$\begin{bmatrix} N^* \\ 0 \\ 0 \end{bmatrix}$	$\begin{bmatrix} 0 \\ E^* \\ 0 \end{bmatrix}$	$\begin{bmatrix} 0 \\ 0 \\ V^* \end{bmatrix}$
$\underline{m}$	$\begin{bmatrix} 1 \\ 0 \\ 0 \end{bmatrix}$	$\begin{bmatrix} 0 \\ 1 \\ 0 \end{bmatrix}$	$\begin{bmatrix} 0 \\ 0 \\ 1 \end{bmatrix}$

Turning Point. In horizontal wells, the trajectory is steered to remain in the reservoir section, successively building and dropping inclination to avoid breaching the bottom or top of the pay zone. The calculation of the turning points, at which the well becomes horizontal, is of interest from a reservoir perspective (see **Fig. 8**). Because these points represent the maximum and minimum vertical depths, they are also needed to determine the numerical range of axes in well plots.

This case is equivalent to interpolating on an inclination. In this special case, direct determination of the azimuth ϕ^* at the turning point is possible according to Eq. 31:

$$\phi^* = \tan^{-1}\left(\frac{\cos\theta_1 \sin\theta_2 \sin\phi_2 - \cos\theta_2 \sin\theta_1 \sin\phi_1}{\cos\theta_1 \sin\theta_2 \cos\phi_2 - \cos\theta_2 \sin\theta_1 \cos\phi_1}\right). \quad \ldots\ldots (31)$$

In deriving Eq. 31, it is assumed that $\theta_1 < \theta_2$, and so represents a minimum inclination. Should $\theta_1 > \theta_2$, then the inclination is a maximum. In this case, the direction of $\underline{t}^*$ will change by π, and the azimuth becomes $(\phi^* + \pi)$. The course length S^* to the turning point can then be calculated from the relationship $S^* = S_{12}\alpha^*/\alpha$. Finally, its position, vector $\underline{p}^*$, can be calculated using the $\underline{t}_1$ and $\underline{t}^*$ vectors with the minimum curvature equation (Eq. 11); refer to the Appendix (Eqs. A-44 through A-46).

Position at Target Defined. Hogg and Thorogood[15] described expressions for the minimum curvature and minimum distance from a point $\underline{p}_1$ on a wellbore, with direction $\underline{t}_1$ to a target $\underline{p}_3$ (see **Fig. 9**).

Their algorithms were iterative and depended on the explicit determination of the center of the curvature of the arc, which causes problems for small angle changes. The Appendix (Eqs. A-47 through A-64) shows how the minimum curvature and minimum distance can be determined explicitly, without reference to the center of the curvature. For a fixed radius of curvature, there

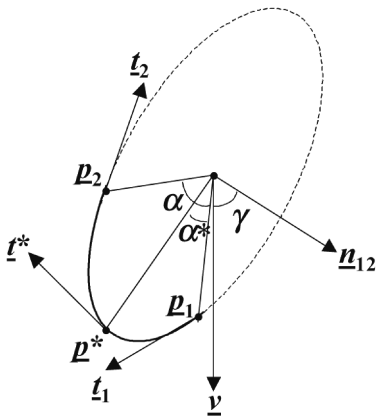

Fig. 8—The turning point $\underline{p}^*$ is the point at which the well becomes horizontal.

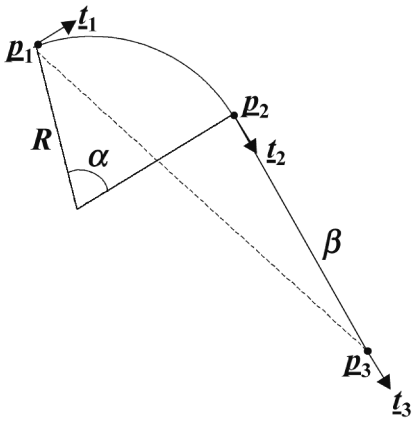

Fig. 9—In general, one curved and one straight section are required if only the position $\underline{p}_3$ of the target is defined.

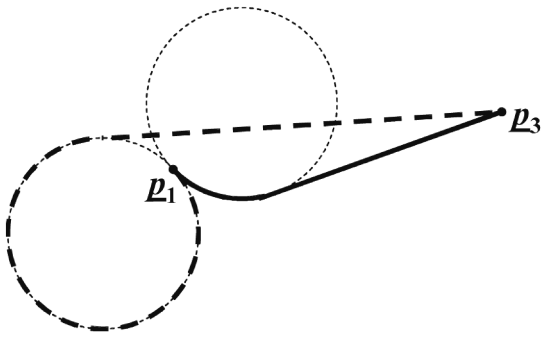

Fig. 10—For a fixed radius of curvature, there are two possible trajectories from $\underline{p}_1$ to $\underline{p}_3$.

are two possible trajectories from $\underline{p}_1$ to $\underline{p}_3$, shown by the solid and dashed lines in **Fig. 10.** All the trajectories lie in a plane. The solid line shows the minimum distance to the target. The other trajectory, shown by the dashed line, requires an angle change greater than π.

The changes in angle can be categorized according to the position of the target point $\underline{p}_3$, relative to the starting point $\underline{p}_1$ and the direction $\underline{t}_1$. These categories are represented by the Regions A through F in **Fig. 11.** Targets falling in Region A can be hit with angle changes less than $\pi/2$ (90°); B, with angle changes less than π (180°); C, with angle changes less than $3\pi/2$ (270°); and D, with angle changes less than 2π (360°). Areas E and F cannot be hit at the prescribed buildup rate.

The appropriate region is determined by calculating the distance, ψ, between the points $\underline{p}_1$ and $\underline{p}_3$; the perpendicular distance, η, from $\underline{p}_1$ in the direction $\underline{t}_1$; and the distance, ξ, normal to $\underline{t}_1$, in Eqs. 32, 33, and 34, respectively; refer to **Fig. 12:**

$$\psi^2 = \left|\underline{p}_3 - \underline{p}_1\right|^2, \quad \ldots\ldots (32)$$

$$\eta = (\underline{p}_3 - \underline{p}_1) \cdot \underline{t}_1, \quad \ldots\ldots (33)$$

$$\xi = (\psi^2 - \eta^2)^{\frac{1}{2}}. \quad \ldots\ldots (34)$$

From Fig. 11 it can be seen that if $\eta \le 0$ and $\xi \le 2R$, then $\alpha \ge \pi$, which is outside the imposed limit on the angle change. With the restriction $0 \le \alpha < \pi$, only targets in areas A, B, and E apply.

Minimum Distance to Target. If $R^2 < \psi^2 + \eta^2$, then the tangent-section length, β, is greater than 0. Because of the imposed restriction $0 \le \alpha < \pi$, the target must be in Region A or B (see Fig. 11). The values of the tangent-section length and angle change, corresponding to the minimum distance to the target, are calculated with Eqs. 35 and 36, respectively:

$$\beta = [\psi^2 - 2R(\psi^2 - \eta^2)^{\frac{1}{2}}]^{\frac{1}{2}} \quad \ldots\ldots (35)$$

and

$$\alpha = 2\tan^{-1}\left[\frac{\eta - \beta}{2R - (\psi^2 - \eta^2)^{\frac{1}{2}}}\right]. \quad \ldots\ldots (36)$$

The course length is then calculated as $S_{12} = R\alpha$. In straight hole, $\psi = \eta$ and, as long as R is finite, Eq. 35 reduces to the distance between the points $\underline{p}_3$ and $\underline{p}_1$. The straight-hole case, therefore, degenerates to a straight line, rather than an arc with an infinitely large radius, conferring stability to the calculation. Finally, $\underline{t}_2$ is calculated using Eq. 37:

$$\underline{t}_2 = \frac{\underline{p}_3 - \underline{p}_1 - \frac{S_{12} f(\alpha)}{2}\underline{t}_1}{\frac{S_{12} f(\alpha)}{2} + \beta}. \quad \ldots\ldots (37)$$

Minimum Curvature to Target. If $R^2 \ge \psi^2 + \eta^2$, then the target must lie in Region E and the build rate is insufficient to hit it. To hit the target, the build rate must be increased to the critical radius of curvature R_c, given by Eq. 38. The corresponding angle change, α_c, is given by Eq. 39.

$$R_c = \frac{\psi^2}{2(\psi^2 - \eta^2)^{\frac{1}{2}}}, \quad \ldots\ldots (38)$$

$$\alpha_c = 2\tan^{-1}\left[\frac{(\psi^2 - \eta^2)^{\frac{1}{2}}}{\eta}\right]. \quad \ldots\ldots (39)$$

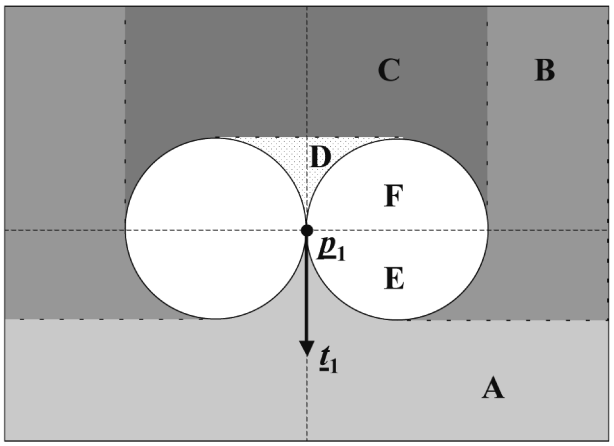

Fig. 11—The regions A through F are defined by the total change in angle.

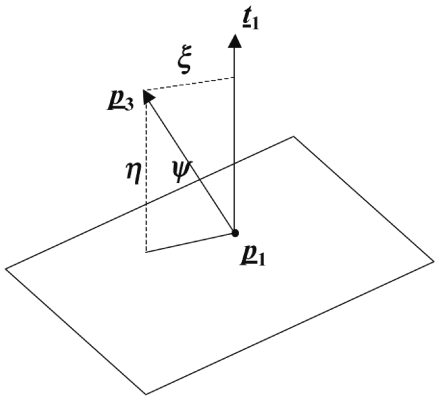

Fig. 12—Graphical realization of the η and ξ variables.

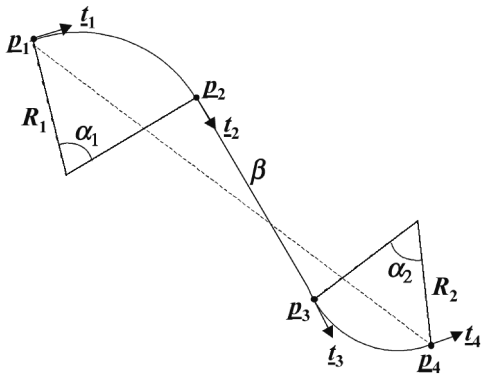

Fig. 13—In general, two curved and one straight section are required if both the position $\underline{p}_4$ and direction $\underline{t}_4$ at the target are defined.

The course length can be calculated as $S_{12} = R_c\alpha_c$. Finally, $\underline{t}_2$ is calculated from Eq. 37 with the tangent-section length, β, equal to 0.

Position and Direction at Target Defined. Advances in surveying and geosteering techniques have enabled multiple targets to be penetrated as a matter of course. The targets may be at different geological horizons or different fault blocks in the same horizon. In these cases, the well's trajectory must be lined up and its direction on entry to or exit from the target must be defined, as well as its position. The trajectory can no longer be achieved with a simple build-and-hold profile. An additional curved section must be added, and in general, the trajectory is 3D (see **Fig. 13**). However, because the target can be specified so that the trajectory lies completely in a plane, this calculation can also be used to design nudge profiles to increase well separation directly beneath a well cluster. Liu and Shi[16,17] described an iterative scheme using coordinate transforms for the solution of the equations. Different calculations were used for each of the two arcs.

We offer an alternate iterative solution on the basis of the geometrical symmetry of the problem and the minimum distance-to-target scheme described earlier in this paper. The advantage of this scheme is that only the subtended angles, α_1 and α_2, of the arcs need to be determined at each iteration. Inspection of Fig. 13 shows that, in general, each of the two sets of points ($\underline{p}_1$, $\underline{p}_2$, $\underline{p}_3$ and $\underline{p}_2$, $\underline{p}_3$, $\underline{p}_4$) are geometrically similar. This suggests applying the minimum distance-to-target algorithm alternately for each of the sets of points.

Let $\underline{p}_{1,j}$ and $\underline{p}_{4,j}$ be the targets and $\alpha_{1,j}$ and $\alpha_{2,j}$ be the subtended angles at the jth iteration. To start the scheme, the subtended angle $\alpha_{1,0}$ is calculated using the minimum distance-to-target algorithm between the points $\underline{p}_1$ and $\underline{p}_4$. This corresponds to Trajectory 1 in **Fig. 14.**

A new target, $\underline{p}_{1,1}$, is calculated with Eq. 40:

$$\underline{p}_{1,j+1} = \underline{p}_1 + R_1 \tan\left(\frac{\alpha_{1,j}}{2}\right)\underline{t}_1. \quad \ldots\ldots\ldots\ldots\ldots\ldots\ldots\ldots (40)$$

The subtended angle, $\alpha_{2,0}$, is now calculated for the second arc, using the points $\underline{p}_4$ and $\underline{p}_{1,1}$. When performing the calculation, the direction of the borehole at $\underline{p}_4$ must be set to $-\underline{t}_4$, to calculate the correct angle. This corresponds to Trajectory 2 in Fig. 14. A new target, $\underline{p}_{4,1}$, is calculated with Eq. 41, which completes the first iteration:

$$\underline{p}_{4,j+1} = \underline{p}_4 - R_2 \tan\left(\frac{\alpha_{2,j}}{2}\right)\underline{t}_4. \quad \ldots\ldots\ldots\ldots\ldots\ldots\ldots\ldots (41)$$

The next iteration is started by calculating the subtended angle, $\alpha_{1,1}$, using the points $\underline{p}_1$, and $\underline{p}_{4,1}$, and so on. Iteration continues until the desired precision is achieved. A suitable criterion for convergence is given by Eq. 42:

$$\varepsilon > [(\alpha_{1,j+1} - \alpha_{1,j})^2 + (\alpha_{2,j+1} - \alpha_{2,j})^2]^{\frac{1}{2}}. \quad \ldots\ldots\ldots\ldots\ldots\ldots\ldots\ldots (42)$$

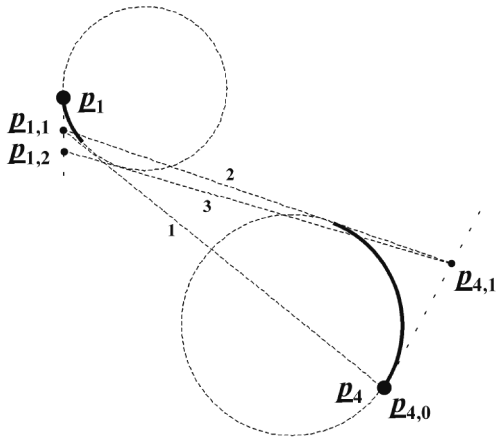

Fig. 14—The iterative scheme used to calculate the trajectory, if both the position and direction at the target are defined.

Four iterations are usually sufficient to reduce the error, ε, below 10^{-5} radians. Note that on completing the calculation, the direction vectors of the second build-and-hold trajectory must be reversed before use.

From a safety-critical-systems perspective, neither the above scheme nor that proposed by Liu and Shi[16] are completely satisfactory. In neither case is convergence proved, and no definitive statement is made regarding the conditions under which no solutions exist (e.g., when the radii of curvature are too large to hit the target). Further work is required.

Closest Approach. The calculation of the closest distance of a point $\underline{p}_x$ to a circular arc (see **Fig. 15**) is the key to the construction of the normal plane collision-avoidance diagram described by Thorogood and Sawaryn.[18]

The closest approach is reached when the vector ($\underline{p}_x$–$\underline{p}$*) is normal to the curve. The subtended angle, α*, to this point is calculated using Eqs. 43 through 45:

$$\eta_1 = (\underline{p}_x - \underline{p}_1) \cdot \underline{t}_1, \quad \ldots\ldots\ldots\ldots\ldots\ldots\ldots\ldots\ldots\ldots (43)$$

$$\eta_2 = (\underline{p}_x - \underline{p}_1) \cdot \underline{t}_2, \quad \ldots\ldots\ldots\ldots\ldots\ldots\ldots\ldots\ldots\ldots (44)$$

$$\alpha^* = \tan^{-1}\left[\eta_1 \Big/ \left(\frac{\eta_1\cos\alpha - \eta_2}{\sin\alpha} + \frac{S_{12}}{\alpha}\right)\right]. \quad \ldots\ldots\ldots\ldots (45)$$

The corresponding position $\underline{p}$* on the arc is determined by interpolating on the subtended angle α*, and then using the minimum curvature equation. Finally, the distance is calculated from the magnitude of the vector ($\underline{p}_x$–$\underline{p}$*). Mathematical and practical difficulties arise when the distance to the point is of the same magnitude or exceeds the radius of the curvature of the arc. Further discussion on this topic may become available in future publications.

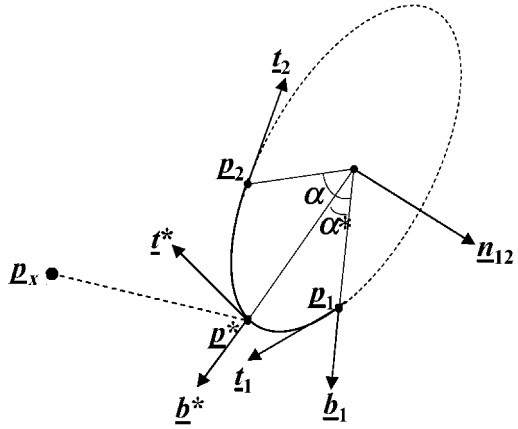

Fig. 15—The closest approach of a point $\underline{p}_x$ to a circular arc.

Straight-Hole Conditions. Eq. 45 is indeterminate in straight hole when α equals 0. For $\alpha<10^{-4}$ radians, small-angle approximations are used, and Eq. 46 is used to calculate the course length, S^*, directly:

$$S^* \approx \frac{S_{12}\eta_1}{\eta_1 - \eta_2 + S_{12}}. \quad \ldots\ldots\ldots\ldots\ldots\ldots\ldots\ldots\ldots\ldots (46)$$

The point $\underline{p}^*$ is calculated by interpolating on measured depth, assuming straight-hole conditions. For these very small, subtended angles, the value of the shape factor $f(\alpha^*)$ in the minimum curvature equation equals unity. Again, the distance is calculated from the magnitude of the vector $(\underline{p}_x - \underline{p}^*)$.

Toolface Angle. Liu and Shi[16] provided useful expressions for the toolface at the start and end of the arc, in terms of the inclination and azimuth values at its ends. The Appendix (Eqs. A-66 through A-79) shows how the general vector equation provided by Thorogood and Sawaryn[18] may be expanded in terms of the inclination and azimuth values at any intermediate point on the arc, as well as at its ends (Eq. 47):

$$\tan\tau^* = \frac{\sin\theta^*[\sin\theta_2 \cos\alpha^* \sin(\phi_2 - \phi^*) + \sin\theta_1 \cos(\alpha - \alpha^*)\sin(\phi^* - \phi_1)]}{\cos(\alpha - \alpha^*)\cos\theta_1 - \cos\alpha^* \cos\theta_2}. \quad \ldots\ldots\ldots\ldots\ldots\ldots (47)$$

At the ends, this expression reduces to those presented by Liu and Shi.[16] Eqs. 48 and 49 have a small advantage because they are not singular when the inclination at either of the ends is zero. Dividing both numerator and denominator by a factor that can be zero causes the singularity.

$$\tau_1 = \tan^{-1}\left[\frac{\sin\theta_2 \sin(\phi_2 - \phi_1)}{\sin\theta_2 \cos\theta_1 \cos(\phi_2 - \phi_1) - \sin\theta_1 \cos\theta_2}\right] \quad \ldots\ldots (48)$$

and

$$\tau_2 = \tan^{-1}\left[\frac{\sin\theta_1 \sin(\phi_2 - \phi_1)}{\sin\theta_2 \cos\theta_1 - \sin\theta_1 \cos\theta_2 \cos(\phi_2 - \phi_1)}\right]. \quad \ldots\ldots (49)$$

Straight-Hole Conditions. For $\alpha<10^{-4}$ radians, small-angle approximation to Eq. 47 is used, giving Eq. 50. The toolface is constant over the arc and is undefined when $\alpha = 0$. If the azimuth values in Eq. 50 straddle north, the minimum angular difference should be used:

$$\tan\tau^* \approx \sin\theta_1\left(\frac{\phi_2 - \phi_1}{\theta_2 - \theta_1}\right). \quad \ldots\ldots\ldots\ldots\ldots\ldots\ldots\ldots\ldots\ldots (50)$$

Curvature. The total curvature, κ, is a constant $1/R$ on a circular arc (see **Fig. 16**). Liu and Shi[16] presented expressions for the inclination and azimuthal components of the curvature at any point on an arc, in terms of the toolface angle at its start.

Using vector methods, the inclination and azimuthal curvatures can be shown to be Eqs. 51 and 52, respectively. The signed values of these expessions are commonly referred to as the build rate and walk rate, respectively. For further details, see the Appendix (Eqs. A-79 through A-81). These two components satisfy Wilson's[19] expression (Eq. 53) for the total curvature κ:

$$\kappa_\theta^* = \kappa\left|\cos\tau^*\right|, \quad \ldots\ldots\ldots\ldots\ldots\ldots\ldots\ldots\ldots\ldots\ldots\ldots (51)$$

$$\kappa_\phi^* = \kappa\left|\frac{\sin\tau^*}{\sin\theta^*}\right|, \quad \ldots\ldots\ldots\ldots\ldots\ldots\ldots\ldots\ldots\ldots\ldots\ldots (52)$$

and

$$\kappa = (\kappa_\theta^{*2} + \kappa_\phi^{*2} \sin^2\theta^*)^{\frac{1}{2}}. \quad \ldots\ldots\ldots\ldots\ldots\ldots\ldots\ldots\ldots\ldots\ldots (53)$$

Eqs. 51 and 52 can be used to derive the equivalents (Eqs. 54 and 55) of Liu and Shi's[16] expressions. The representation of the azimuthal component is simplified:

$$\kappa_\theta^* = \kappa\left|\frac{\cos(\alpha - \alpha^*)\cos\theta_1 - \cos\alpha^* \cos\theta_2}{\sin\alpha \sin\theta^*}\right| \quad \ldots\ldots\ldots\ldots\ldots (54)$$

and

$$\kappa_\phi^* = \kappa\left|\frac{\sin\theta_2 \cos\alpha^* \sin(\phi_2 - \phi^*) + \sin\theta_1 \cos(\alpha - \alpha^*)\sin(\phi^* - \phi_1)}{\sin\alpha \sin\theta^*}\right| \quad \ldots\ldots\ldots\ldots\ldots\ldots\ldots (55)$$

Straight-Hole Conditions. Again, for $\alpha<10^{-4}$ radians, small-angle approximations to Eqs. 54 and 55 are used, and Eqs. 56 and 57 are used to calculate the curvatures. If the azimuth values in Eq. 57 straddle north, the minimum angular difference should be used:

$$\kappa_\theta^* \approx \frac{\left|\theta^* - \theta_1\right|}{S^*} \approx \frac{\left|\theta_2 - \theta_1\right|}{S_{12}}, \quad \ldots\ldots\ldots\ldots\ldots\ldots\ldots\ldots\ldots\ldots (56)$$

and

$$\kappa_\phi^* \approx \frac{\left|\phi^* - \phi_1\right|}{S^*} \approx \frac{\left|\phi_2 - \phi_1\right|}{S_{12}}. \quad \ldots\ldots\ldots\ldots\ldots\ldots\ldots\ldots\ldots\ldots (57)$$

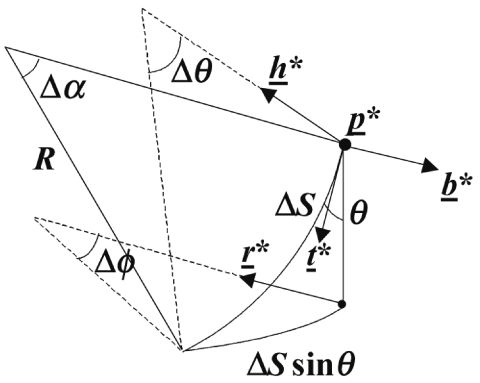

Fig. 16—The principal curve, inclination, and azimuthal components.

Implementation and Testing

The algorithms in this paper are presented in logical order with the later, more-complex cases using results of earlier ones. It is recommended that the routines are coded and tested in this order. All the equations required for successful implementation are contained in the body of the paper.

Once coded, a good test procedure is to calculate values in two different ways. For example, a point can be interpolated using each of the following: measured depth, inclination, and azimuth determined from the previous calculation in cyclic order. The results should be identical. The four-point trajectory presented in **Table 2** is constructed with both the wellbore position and direction at the target defined. This example can be used to test most of the algorithms presented here. Station numbers with alphabetical suffixes indicate interpolated points. Williamson[8] presents other trajectories that may be used as tests in both oilfield and metric units.

Conclusions

1. Previously unpublished algorithms have been presented for small-angle approximations associated with a circular arc, the determination of a turning point, a general expression for toolface angle, and the minimum distance to a target with and without the direction at the target defined.
2. Vector methods are useful tools for 3D-directional calculations and often result in simpler expressions compared to other means. Their use is recommended.
3. A standard nomenclature is required for all directional work that is compatible with other related subject areas, such as survey-instrument design and terrestrial surveying. Consistency with accepted mathematical conventions in vector calculus should also be reviewed.
4. The point-to-target algorithm, with both position and direction at the target defined, is the only construction presented in this

TABLE 2—TEST CASE BASED ON A TRAJECTORY WITH BOTH ITS POSITION AND DIRECTION DEFINED AT THE TARGET

No.	Measured Depth (ft)	Inclination (deg)	Azimuth (deg)	N (ft)	E (ft)	V (ft)	Dogleg Severity (deg/100ft)	τ (deg)	κ_θ (deg/100ft)	κ_ϕ (deg/100ft)	κ (deg/100ft)	R (ft)
1	702.55	5.50	45.00	40.00	40.00	700.00	—	38.14	1.57	12.89	2.00	2,864.78
2	1,964.57	29.75	77.05	154.78	393.64	1,895.35	2.00	6.85	1.99	0.48	2.00	2,864.78
2a	4,250.00	29.75	77.05	408.84	1,498.82	3,879.60	0.00	—	—	—	—	—
3	5,086.35	29.75	77.05	501.82	1,903.25	4,605.73	0.00	-135.72	2.15	4.22	3.00	1,909.85
3a	8,504.11	80.89	300.71	1,967.04	1,033.30	7,050.00	3.00	-20.54	2.81	1.07	3.00	1,909.85
3b	8,828.04	90.00	297.31	2,123.40	751.22	7,075.71	3.00	-20.27	2.81	1.04	3.00	1,909.85
3c	9,151.97	99.11	293.92	2,262.88	460.41	7,050.00	3.00	-20.54	2.81	1.07	3.00	1,909.85
4	9,901.68	120.00	285.00	2,500.00	-200.00	6,800.00	3.00	-23.58	2.75	1.39	3.00	1,909.85

paper for which an explicit solution has not been found. Also, the conditions under which no solutions are possible should be identified (e.g., when the radii of curvature are too large to hit the target). Further work is needed.

5. Increasingly complex trajectory plans emerging from work on designer wells means segments of the well plan may exceed 180° and the alternative solutions may need to be considered.
6. The simple representation afforded by the circular-arc construct allows for a consistent treatment of the associated mathematical operations. Representation of the wellbore path in a different form (for example, a spline or polynomial) would necessitate rederivation of all the constructs in this paper. This may not be a simple task.

Nomenclature

A = constant
$\underline{b}$ = negative unit normal vector
B = constant
c = a function of the ratio of the course lengths S^*/S_{12} on an arc
C = constant
D = measured depth, L, ft
E = easting, L, ft
f = geometrical shape factor
$\underline{h}$ = unit highside vector
$\underline{m}$ = unit vector normal to a plane
$\underline{n}$ = unit binormal vector
N = northing, L, ft
$\underline{p}$ = position vector in N,E,V coordinates, L, ft
$\underline{r}$ = unit rightside vector
R = radius of curvature, L, ft
S = course length, L, ft
$\underline{t}$ = unit direction vector
$\underline{v}$ = unit vertical vector in N,E,V coordinates, L, ft
V = vertical, L, ft
z = dummy angle, radians
α = subtended angle, radians
β = length of the tangent section, L, ft
γ = angle between the binormal and vertical vectors, radians
ε = angular-error tolerance, radians
ζ = substituted variable
η = substitution for a dot product, L, ft
θ = inclination angle, radians
κ = curvature, radians/L, radians/ft
ξ = substitution for a dot product, L, ft
τ = toolface angle, radians
ϕ = azimuth angle, radians
ψ = substitution for a dot product, L, ft
Δ = a difference in a parameter
Θ = dip angle, radians
Φ = dip azimuth, radians

Subscripts and Superscripts

c = critical value
j = iteration counter
x = position of a defining point
1,2,3,4 = first, second, third or fourth point, arc, or property
θ = inclination component
ϕ = azimuthal component
$*$ = component to be determined

Acknowledgment

The authors thank BP plc for permission to publish this paper.

References

1. Mason, C.M. and Taylor, H.L.: "A Systematic Approach to Well Surveying Calculations," *SPEJ* (June 1971).
2. Zaremba, W.A.: "Directional Survey by The Circular-Arc Method," *SPEJ* (February 1973) 5; *Trans.*, AIME, **255.**
3. *Bull. D20, Directional Drilling Survey Calculation Methods and Terminology*, first edition, API, Dallas (December 1985).
4. Walstrom, J.E., Harvey R.P., and Eddy H.D.: "A Comparison of Various Directional Survey Models and an Approach To Model Error Analysis," *JPT* (August 1972) 935.
5. Sawaryn, S.J., Sanstrom, W., and McColpin, G.: "The Management of Drilling Engineering and Well Services Software as Safety Critical Systems," paper SPE 73893 presented at the 2002 SPE International Conference on Health, Safety, and Environment in Oil and Gas Exploration and Production, Kuala Lumpur, 20–22 March.
6. Sawaryn, S.J. *et al.:* "Safety Critical Systems Principles Applied to Drilling Engineering and Well Services Software," paper SPE 84152 presented at the 2003 SPE Annual Technical Conference and Exhibition, Denver, 5–8 October.
7. *Delivery Update—Autotrack Milestones,* Baker Hughes Inteq, Tananger, Norway (2002) 18.
8. Williamson, H.S.: "Accuracy Prediction for Directional Measurement While Drilling," *SPEDC* (December 2000) 221.
9. *SPE Letter and Computer Symbols Standard,* SPE, Richardson, Texas (1993).
10. Williamson, H.S. and Wilson, H.F.: "Directional Drilling and Earth Curvature," *SPEDC* (March 2000).
11. Stockhausen, E.J. and Lesso, W.G.: "Continuous Direction and Inclination Measurements Lead to an Improvement in Wellbore Positioning," paper SPE/IADC 79917 presented at the 2003 SPE/IADC Drilling Conference, Amsterdam, 19–21 February.
12. Thorogood, J.L.: "Well Surveying Data," *World Oil Magazine* (April 1986) 100.
13. Knuth, D.E.: *The Art of Computer Programming Volume 2: Seminumerical Algorithm,* third edition, Addison Wesley (1997) 485–488.
14. Wolfram Research, *Mathematica 4 Standard Add-On Packages,* Wolfram Media Inc., Champaign, Illinois (1999) 34.
15. Hogg, T.W. and Thorogood, J.L.: "Performance Optimization of Steerable Systems," ASME Energy Resources Technology Conference, New Orleans (January 1990) 49–58.
16. Liu, X. and Shi, Z.: "Improved Method Makes a Soft Landing of Well Path," *Oil & Gas J.* (October 2001) 48.

17. Liu, X. and Jun, G.: "Description and Calculation of the Well Path with Spatial Arc Model," *Natural Gas Industry,* Beijing (2000) **20,** No. 5, 44–47.
18. Thorogood, J.L. and Sawaryn, S.J.: "The Travelling-Cylinder Diagram: A Practical Tool for Collision Avoidance," *SPEDE* (March 1991) 31.
19. Wilson, G.J.: "An Improved Method for Computing Directional Surveys," *JPT* (August 1968) 871.
20. Weatherburn, C.E.: *Elementary Vector Analysis,* G. Bell and Sons, London (1967).
21. Abramowitz and Stegun: *Handbook of Mathematical* Functions, Dover, New York City (1972) 75.

Appendix

Summary of Vector Methods. Weatherburn[20] presents details of all vector methods used in this paper. The key constructions are the dot, or scalar, product (·) and vector cross product (×). Let a_1, a_2, a_3; b_1, b_2, b_3; and c_1, c_2, c_3 be the N,E,V components of vectors $\underline{a}$, $\underline{b}$, and $\underline{c}$, respectively. Let α be the angle between the $\underline{a}$ and $\underline{b}$ vectors, and $\underline{n}$ be a unit vector normal to both $\underline{a}$ and $\underline{b}$. The dot and cross products are then described by Eqs. A-1 through A-3:

$$\underline{a} \cdot \underline{b} = a_1 b_1 + a_2 b_2 + a_3 b_3, \quad \text{(A-1)}$$

$$\underline{a} \cdot \underline{b} = |\underline{a}|\,|\underline{b}| \cos\alpha, \quad \text{(A-2)}$$

$$\underline{a} \times \underline{b} = |\underline{a}|\,|\underline{b}| \sin\alpha\, \underline{n}, \quad \text{(A-3)}$$

$$\underline{a} \times (\underline{b} \times \underline{c}) = (\underline{a} \cdot \underline{c})\underline{b} - (\underline{a} \cdot \underline{b})\underline{c}, \quad \text{(A-4)}$$

$$\underline{a} \cdot (\underline{b} \times \underline{c}) = a_1(b_2c_3 - b_3c_2) + a_2(b_3c_1 - b_1c_3) + a_3(b_1c_2 - b_2c_1). \quad \text{(A-5)}$$

Minimum Curvature. Zaremba[2] presented the following derivation (refer to Fig. 4, the direction vectors $\underline{t}_1$ and $\underline{t}_2$ at the arc's ends are given by Eqs. A-6 and A-7, respectively):

$$\underline{t}_1 = \begin{bmatrix} \sin\theta_1 \cos\phi_1 \\ \sin\theta_1 \sin\phi_1 \\ \cos\theta_1 \end{bmatrix} \quad \text{(A-6)}$$

and

$$\underline{t}_2 = \begin{bmatrix} \sin\theta_2 \cos\phi_2 \\ \sin\theta_2 \sin\phi_2 \\ \cos\theta_2 \end{bmatrix} \quad \text{(A-7)}$$

The binormal vector, $\underline{n}_{12}$, and vectors $\underline{b}_1$ and $\underline{b}_2$ at the arc's ends, are given by the Eqs. A-8, A-9, and A-10, respectively:

$$\underline{n}_{12} = \frac{\underline{t}_1 \times \underline{t}_2}{\sin\alpha}, \quad \text{(A-8)}$$

$$\underline{b}_1 = \underline{t}_1 \times \underline{n}_{12}, \quad \text{(A-9)}$$

and

$$\underline{b}_2 = \underline{t}_2 \times \underline{n}_{12}. \quad \text{(A-10)}$$

Substituting $\underline{n}_{12}$ from Eq. A-8 into Eqs. A-9 and A-10, and using Eq. A-4 for the vector triple products, gives Eqs. A-11 and A-12:

$$\underline{b}_1 = \frac{\underline{t}_1 \cos\alpha - \underline{t}_2}{\sin\alpha} \quad \text{(A-11)}$$

and

$$\underline{b}_2 = \frac{\underline{t}_1 - \underline{t}_2 \cos\alpha}{\sin\alpha}. \quad \text{(A-12)}$$

The position $\underline{p}_2$ is calculated from $\underline{p}_1$ using Eq. A-13. Substituting $\underline{b}_1$ and $\underline{b}_2$ from Eqs. A-11 and A-12 into Eq. A-13 gives Eq. A-14:

$$\underline{p}_2 = \underline{p}_1 + R(\underline{b}_2 - \underline{b}_1) \quad \text{(A-13)}$$

$$\underline{p}_2 = \underline{p}_1 + R\frac{(1 - \cos\alpha)}{\sin\alpha}(\underline{t}_1 + \underline{t}_2). \quad \text{(A-14)}$$

Finally, recalling the trigonometric identity $\tan(\alpha/2) = (1 - \cos\alpha)/\sin\alpha$, and that $S_{12} = R\alpha$, we obtain the now familiar expression for the minimum curvature equation:

$$\underline{p}_2 = \underline{p}_1 + \frac{S_{12}}{\alpha}\tan\left(\frac{\alpha}{2}\right)(\underline{t}_1 + \underline{t}_2). \quad \text{(A-15)}$$

Straight-Hole Conditions. For small angles, $\tan(z)$ can be expanded in a Taylor series,[21] Eq. A-16. Using the first five terms of the expansion, the factor $\tan(\alpha/2)/(\alpha/2)$ can be put into Horner[12,13] form, giving Eq. 12 in the body of the paper:

$$\tan(z) = z + \frac{z^3}{3} + \frac{2z^5}{15} + \frac{17z^7}{315} + \frac{62z^9}{2835} + \quad \text{(A-16)}$$

For small angles, the shape factor can be treated as unity and Eq. A-15 reduces to Eq. A-17, which is recognized as the balanced tangential-survey calculation method[3]:

$$\underline{p}_2 \approx \underline{p}_1 + \frac{S_{12}}{2}(\underline{t}_1 + \underline{t}_2). \quad \text{(A-17)}$$

Interpolation. Referring to Fig. 6, interpolation involves determining the position $\underline{p}^*$ at some point on the arc, given a criterion. The corresponding direction vector at the point is $\underline{t}^*$ (Eq. A-18):

$$\underline{t}^* = \begin{bmatrix} \sin\theta^* \cos\phi^* \\ \sin\theta^* \sin\phi^* \\ \cos\theta^* \end{bmatrix}. \quad \text{(A-18)}$$

The binormal vector, $\underline{n}_{12}$, can also be written in terms of the direction vectors at the start point and the point at which the interpolation is to take place:

$$\underline{n}_{12} = \frac{\underline{t}_1 \times \underline{t}^*}{\sin\alpha^*}. \quad \text{(A-19)}$$

Equating Eqs. A-8 and A-19, and taking the cross product of both sides of the equality with $\underline{t}_1$, gives Eq. A-20:

$$\frac{\underline{t}_1 \times (\underline{t}_1 \times \underline{t}^*)}{\sin\alpha^*} = \frac{\underline{t}_1 \times (\underline{t}_1 \times \underline{t}_2)}{\sin\alpha}. \quad \text{(A-20)}$$

Using Eq. A-4 to expand the triple-cross products, and rearranging for $\underline{t}^*$, gives Eq. A-21:

$$\underline{t}^* = \underline{t}_1 \cos\alpha^* - \frac{\sin\alpha^*(\underline{t}_1 \cos\alpha - \underline{t}_2)}{\sin\alpha}. \quad \text{(A-21)}$$

Multiply the numerator and denominator of the first term in A-21 by $\sin\alpha$ and collect terms in $\underline{t}_1$ and $\underline{t}_2$. After simplification, this gives the important relationship in A-22 that is the foundation for all the interpolation formulae:

$$\underline{t}^* = \frac{\sin(\alpha - \alpha^*)}{\sin\alpha}\underline{t}_1 + \frac{\sin\alpha^*}{\sin\alpha}\underline{t}_2. \quad \text{(A-22)}$$

Substituting Eqs. A-6, A-7, and A-18 into Eq. A-22 gives Eq. A-23:

$$\begin{bmatrix} \sin\theta^* \cos\phi^* \\ \sin\theta^* \sin\phi^* \\ \cos\theta^* \end{bmatrix} = \frac{\sin(\alpha - \alpha^*)}{\sin\alpha}\begin{bmatrix} \sin\theta_1 \cos\phi_1 \\ \sin\theta_1 \sin\phi_1 \\ \cos\theta_1 \end{bmatrix} + \frac{\sin\alpha^*}{\sin\alpha}\begin{bmatrix} \sin\theta_2 \cos\phi_2 \\ \sin\theta_2 \sin\phi_2 \\ \cos\theta_2 \end{bmatrix}. \quad \text{(A-23)}$$

Interpolation on Measured Depth. Because the radius of the arc is fixed, the ratio of the subtended angles is identical to the ratio of the course lengths to the same points, as shown in Eq. A-24:

$$\frac{\alpha^*}{\alpha} = \frac{S^*}{S_{12}}. \quad \text{(A-24)}$$

Substituting α^* from Eq. A-24 into Eq. A-22, gives Eq. A-25 for $\underline{t}^*$, in terms of the course lengths:

$$\underline{t}^* = \frac{\sin\left[\left(1-\frac{S^*}{S_{12}}\right)\alpha\right]}{\sin\alpha}\underline{t}_1 + \frac{\sin\left(\frac{S^*}{S_{12}}\alpha\right)}{\sin\alpha}\underline{t}_2. \quad \text{(A25)}$$

For small values of α, Eq. A-25 can be expanded in a Taylor series. Evaluation of the terms is tedious, and computer assistance[14] was used to establish Eq. 14, presented in the body of the paper. For small angles, the following simple expression can be used:

$$\underline{t}^* \approx \left(1-\frac{S^*}{S_{12}}\right)\underline{t}_1 + \left(\frac{S^*}{S_{12}}\right)\underline{t}_2. \quad \text{(A-26)}$$

Interpolation on Azimuth. Dividing the easting and northing components of Eq. A-23 eliminates $\sin\theta^*$, giving the expression Eq. A-27:

$$\frac{\sin\phi^*}{\cos\phi^*} = \frac{\sin\theta_1\sin\phi_1\sin(\alpha-\alpha^*) + \sin\theta_2\sin\phi_2\sin\alpha^*}{\sin\theta_1\cos\phi_1\sin(\alpha-\alpha^*) + \sin\theta_2\cos\phi_2\sin\alpha^*}. \quad \text{(A-27)}$$

Next, expand the terms $\sin(\alpha-\alpha^*)$ in both numerator and the denominator of Eq. A-25 by use of the trigonometric identity: $\sin(\alpha-\alpha^*) = \sin\alpha\cos\alpha^* - \sin\alpha^*\cos\alpha$. The terms involving $\sin\alpha^*$ are then collected on the left side of the equals sign, and terms involving $\cos\alpha^*$ are collected on the right side. The azimuth terms are then combined by use of the same trigonometric identity to give Eq. 15 for α^*, which was used to interpolate on azimuth in the body of the paper. The traditional form of the dogleg-severity equation[3] Eq. A-28 can be used to determine θ^*. This is in the form of $C = A\sin(\theta^*) + B\cos(\theta^*)$:

$$\cos\alpha^* = \sin\theta_1\cos(\phi^*-\phi_1)\sin\theta^* + \cos\theta_1\cos\theta^*. \quad \text{(A-28)}$$

If the arc lies in the vertical plane, then $(\underline{v}\cdot\underline{n}_{12})$ equals 0, and the solution is single valued. The vector $\underline{n}_{12}$ is given by Eq. A-8. Expanding the scalar triple product using Eq. A-5 gives the expression

$$\frac{\sin\theta_1\sin\theta_2\sin(\phi_2-\phi_1)}{\sin\alpha} = 0. \quad \text{(A-29)}$$

Interpolation on Inclination. Extracting and rearranging the vertical component of Eq. A-23 gives Eq. A-30, which is of the form $C = A\sin(\alpha^*) + B\cos(\alpha^*)$. Once α^* has been found, the azimuth component is determined from Eq. A-27:

$$\sin\alpha^*\cos\theta^* = (\cos\theta_2 - \cos\alpha\cos\theta_1)\sin\alpha^* + \sin\alpha\cos\theta_1\cos\alpha^*. \quad \text{(A-30)}$$

Interpolation at a Plane. Refering to Fig. 7, Eq. A-14 can be used to calculate the point $\underline{p}^*$ from $\underline{p}_1$. The radius, R, can be expressed as S_{12}/α to give Eq. A-31:

$$\underline{p}^* = \underline{p}_1 + \frac{S_{12}(1-\cos\alpha^*)}{\alpha\sin\alpha^*}(\underline{t}_1 + \underline{t}^*). \quad \text{(A-31)}$$

Now, use Eq. A-21 to substitute for $\underline{t}^*$ in Eq. A-31 to give Eq. A-32:

$$\underline{p}^* = \underline{p}_1 + \frac{S_{12}(1-\cos\alpha^*)}{\alpha\sin\alpha^*}\left[(1+\cos\alpha^*)\underline{t}_1 - \frac{\sin\alpha^*(\underline{t}_1\cos\alpha - \underline{t}_2)}{\sin\alpha}\right]. \quad \text{(A-32)}$$

Now, take the dot product of Eq. A-32, with the normal vector $\underline{m}$ of the plane, and rearrange slightly:

$$\underline{m}\cdot(\underline{p}^* - \underline{p}_1) = \frac{S_{12}(1-\cos\alpha^*)}{\alpha\sin\alpha^*}\left\{(1+\cos\alpha^*)(\underline{m}\cdot\underline{t}_1) - \frac{\sin\alpha^*[(\underline{m}\cdot\underline{t}_1)\cos\alpha - (\underline{m}\cdot\underline{t}_2)]}{\sin\alpha}\right\}. \quad \text{(A-33)}$$

The equation of the plane[20] is given by Eq. A-34, showing $(\underline{m}\cdot\underline{p}_x) = (\underline{m}\cdot\underline{p}^*)$:

$$\underline{m}\cdot(\underline{p}_x - \underline{p}^*) = 0. \quad \text{(A-34)}$$

Eq. A-34 can be used to eliminate $\underline{p}^*$ from Eq. A-33. After rearranging, the resulting expression Eq. A-35, is of the form $C = A\sin(\alpha^*) + B\cos(\alpha^*)$:

$$\frac{\underline{m}\cdot(\underline{p}_x - \underline{p}_1)\alpha\sin\alpha}{S_{12}} + (\underline{m}\cdot\underline{t}_1)\cos\alpha - (\underline{m}\cdot\underline{t}_2) = (\underline{m}\cdot\underline{t}_1)\sin\alpha\sin\alpha^* + [(\underline{m}\cdot\underline{t}_1)\cos\alpha - (\underline{m}\cdot\underline{t}_2)]\cos\alpha^*. \quad \text{(A-35)}$$

Straight-Hole Conditions. For small angles, equation Eq. A-35 is badly behaved. Small-angle approximations must be used, and the interpolation must be conducted with respect to measured depth. The expression Eq. A-17 can be used to calculate the position of $\underline{p}^*$ from $\underline{p}_1$, as shown in Eq. A-36:

$$\underline{p}^* = \underline{p}_1 + \frac{S^*}{2}(\underline{t}_1 + \underline{t}^*). \quad \text{(A-36)}$$

Sustituting Eq. A-26 into Eq. A-36 gives Eq. A-37:

$$\frac{S^{*2}}{2S_{12}}(\underline{t}_2 - \underline{t}_1) + S^*\underline{t}_1 - (\underline{p}^* - \underline{p}_1) = 0. \quad \text{(A-37)}$$

Taking the dot product of Eq. A-37, with the normal vector $\underline{m}$ of the plane, and substituting $(\underline{m}\cdot p_x)$ for $(\underline{m}\cdot p^*)$, as before, gives a quadratic equation (Eq. A-38) in the course length, S^*. Eq. A-38 has the solution Eq. A-39:

$$\frac{(\underline{m}\cdot\underline{t}_2) - (\underline{m}\cdot\underline{t}_1)}{2S_{12}}S^{*2} + (\underline{m}\cdot\underline{t}_1)S^* - \underline{m}\cdot(\underline{p}_x - \underline{p}_1) = 0 \quad \text{(A-38)}$$

and

$$S^* = \frac{-(\underline{m}\cdot\underline{t}_1) \pm \left[(\underline{m}\cdot\underline{t}_1)^2 + \frac{2\underline{m}\cdot(\underline{t}_2-\underline{t}_1)\underline{m}\cdot(\underline{p}_x-\underline{p}_1)}{S_{12}}\right]^{\frac{1}{2}}}{\left[\frac{\underline{m}\cdot(\underline{t}_2-\underline{t}_1)}{S_{12}}\right]}. \quad \text{(A-39)}$$

To simplify the manipulation, define a variable, ζ, according to Eq. A-40. Eq. A-39 can then be written as Eq. A-41:

$$\zeta = \frac{\underline{m}\cdot(\underline{p}_x - \underline{p}_1)[(\underline{m}\cdot\underline{t}_2) - (\underline{m}\cdot\underline{t}_1)]}{S_{12}(\underline{m}\cdot\underline{t}_1)^2} \quad \text{(A-40)}$$

$$S^* = \frac{-(\underline{m}\cdot\underline{t}_1) \pm (\underline{m}\cdot\underline{t}_1)(1+2\varsigma)^{\frac{1}{2}}}{\left[\frac{(\underline{m}\cdot\underline{t}_2) - (\underline{m}\cdot\underline{t}_1)}{S_{12}}\right]}. \quad \text{(A-41)}$$

Because 2ζ is much smaller than unity, the square root may be expanded in a series using the first four terms of the binomial expansion,[21] Eq. A-42, to give Eq. A-43:

$$(1+z)^{\frac{1}{2}} = 1 + \frac{z}{2} - \frac{z^2}{8} + \frac{z^3}{16} - \frac{z^4}{128} + \quad \text{(A-42)}$$

$$S^* \approx \frac{-(\underline{m}\cdot\underline{t}_1) \pm (\underline{m}\cdot\underline{t}_1)\left(1 + \varsigma - \frac{\varsigma^2}{2} + \frac{\varsigma^3}{2}\right)}{\left[\frac{(\underline{m}\cdot\underline{t}_2) - (\underline{m}\cdot\underline{t}_1)}{S_{12}}\right]}. \quad \text{(A-43)}$$

From Eq. A-43, it can be seen that the positive root must be chosen so that the expression degenerates to the straight-line case when ζ equals 0. Factoring Eq. A-43 gives Eq. 29 in the body of the paper.

Turning Point. From Fig. 8, the vector $\underline{t}^*$ can be written as Eq. A-44. The angle between the $\underline{n}_{12}$ and $\underline{v}$ vectors is γ:

$$\underline{t}^* = \frac{\underline{n}_{12}\times\underline{v}}{\sin\gamma}. \quad \text{(A-44)}$$

Using A-8 for $\underline{n}_{12}$, and expanding the resulting vector triple product, gives Eq. A-45:

$$\underline{t}^* = \frac{-(\underline{v}\cdot\underline{t}_2)\underline{t}_1 + (\underline{v}\cdot\underline{t}_1)\underline{t}_2}{\sin\gamma\,\sin\alpha}. \quad \text{(A-45)}$$

Note that $(\underline{v}\cdot\underline{t}_2)=\cos\theta_2$, $(\underline{v}\cdot\underline{t}_1)=\cos\theta_1$, and that $\theta^*=\pi/2$ at the turning point. Using these values and Eqs. A-18, A-6, and A-7 for $\underline{t}^*$, $\underline{t}_1$, and $\underline{t}_2$, respectively, in Eq. A-45 gives Eq. A-46:

$$\begin{bmatrix}\cos\phi^*\\ \sin\phi^*\\ 0\end{bmatrix} = \frac{\cos\theta_1}{\sin\gamma\,\sin\alpha}\begin{bmatrix}\sin\theta_2\cos\phi_2\\ \sin\theta_2\sin\phi_2\\ \cos\theta_2\end{bmatrix} - \frac{\cos\theta_2}{\sin\gamma\,\sin\alpha}\begin{bmatrix}\sin\theta_1\cos\phi_1\\ \sin\theta_1\sin\phi_1\\ \cos\theta_1\end{bmatrix}. \quad \text{(A-46)}$$

Dividing the easting by the northing components gives Eq. 31 in the body of the paper, for the azimuth ϕ^* of the turning point.

Position at Target Defined. In the most general case, the target $\underline{p}_3$ can be hit with one curved section of radius R and one straight section of length β (see Fig. 9). Using Eq. A-15, the position $\underline{p}_3$ of the target can be written as Eq. A-47:

$$\underline{p}_3 = \underline{p}_1 + R\tan\left(\frac{\alpha}{2}\right)(\underline{t}_1+\underline{t}_2) + \beta\underline{t}_2. \quad \text{(A-47)}$$

Taking the dot product of A-47 with $\underline{t}_1$, and also with itself, gives A-48 and A-49, respectively:

$$(\underline{p}_3-\underline{p}_1)\cdot\underline{t}_1 = R\sin\alpha + \beta\cos\alpha \quad \text{(A-48)}$$

and

$$|\underline{p}_3-\underline{p}_1|^2 = 2R^2(1-\cos\alpha) + 2\beta R\sin\alpha + \beta^2. \quad \text{(A-49)}$$

Let

$$\psi^2 = |\underline{p}_3-\underline{p}_1|^2 \quad \text{(A-50)}$$

and

$$\eta = (\underline{p}_3-\underline{p}_1)\cdot\underline{t}_1. \quad \text{(A-51)}$$

Substituting Eq. A-50 into Eq. A-49 and Eq. A-51 into Eq. A-48 gives Eqs. A-52 and A-53, respectively. The variable ξ is determined using Pythagoras's theorem (see Fig. 12).

$$\eta = R\sin\alpha + \beta\cos\alpha \quad \text{(A-52)}$$

and

$$\psi^2 = 2R^2(1-\cos\alpha) + 2\beta R\sin\alpha + \beta^2. \quad \text{(A-53)}$$

Multiplying Eq. A-52 by $2R$ gives Eq. A-53. Rearranging Eq. A-54 gives Eq. A-55:

$$2R^2\sin\alpha + 2\beta R\cos\alpha = 2R\eta \quad \text{(A-54)}$$

and

$$2\beta R\sin\alpha - 2R^2\cos\alpha = \psi^2 - \beta^2 - 2R^2. \quad \text{(A-55)}$$

Squaring both Eqs. A-54 and A-55, and adding the results, eliminates α and results in a quadratic in β^2, as shown in Eq. A-56. Solving the quadratic gives an explicit expression for β (Eq. A-57).

$$\beta^4 - 2\beta^2\psi^2 + (\psi^4 - 4R^2\psi^2 + 4R^2\eta^2) = 0, \quad \text{(A-56)}$$

$$\beta = [\psi^2 \pm 2R(\psi^2-\eta^2)^{\frac{1}{2}}]^{\frac{1}{2}}. \quad \text{(A-57)}$$

Inspecting Eq. A-57, the minimum curvature to target will occur when $\beta=0$ and the radius equals R_c, as shown in Eq. A-58. The negative root of Eq. A-57 is the correct one:

$$R_c = \frac{\psi^2}{2(\psi^2-\eta^2)^{\frac{1}{2}}}. \quad \text{(A-58)}$$

To find the angle α, rearrange Eq. A-52 for β and square the result to give Eq. A-59:

$$\beta^2 = \frac{\eta^2 - 2R\eta\sin\alpha + R^2\sin^2\alpha}{\cos^2\alpha}. \quad \text{(A-59)}$$

The substitution of β from Eq. A-52 and β^2 from Eq. A-59 into Eq. A-53 results in Eq. A-60:

$$\psi^2 = 2R^2(1-\cos\alpha) + \frac{2R\sin\alpha}{\cos\alpha}(\eta - R\sin\alpha) + \frac{\eta^2 - 2R\eta\sin\alpha + R^2\sin^2\alpha}{\cos^2\alpha}. \quad \text{(A-60)}$$

Multiplying by $\cos^2\alpha$ and rearranging terms, gives Eq. A-61. Completing the square on the right side of Eq. A-61 gives Eq. A-62:

$$\psi^2\cos^2\alpha = 2R\eta\sin\alpha(\cos\alpha-1) + \eta^2 + R^2(1+\cos^2\alpha) - 2R^2\cos\alpha \quad \text{(A-61)}$$

$$(\psi^2-\eta^2)\cos^2\alpha = [\eta\sin\alpha - R(1-\cos\alpha)]^2. \quad \text{(A-62)}$$

Taking the square root of Eq. A-62 and rearranging for R results in equation Eq. A-63 in the form of $C=A\sin(\alpha)+B\cos(\alpha)$. The solution of such an equation is given by Eq. 1 in the body of the paper:

$$R = \eta\sin\alpha + [R \pm (\psi^2-\eta^2)^{\frac{1}{2}}]\cos\alpha. \quad \text{(A-63)}$$

After substituting the values of the constants A, B, and C, and comparing the result with Eq. A-57, we obtain the important result $A^2+B^2-C^2=\beta^2$.

Finally, the expression for $\alpha/2$ is given by A-64:

$$\tan\left(\frac{\alpha}{2}\right) = \left[\frac{\eta-\beta}{2R-(\psi^2-\eta^2)^{\frac{1}{2}}}\right]. \quad \text{(A-64)}$$

Setting $\beta=0$ and $R=R_c$ in Eq. A-64, gives Eq. 39 in the body of the paper for the subtended angle, α_c, for the minimum curvature to target.

Toolface Angle. The toolface angle is determined by the dot products between the $-\underline{b}$, $\underline{h}$, and $\underline{r}$ vectors (see Fig. 2).

$$(-\underline{b}^*\cdot\underline{h}^*) = \cos\tau^* \quad \text{(A-65)}$$

and

$$(-\underline{b}^*\cdot\underline{r}^*) = \sin\tau^*. \quad \text{(A-66)}$$

Eqs. A-65 and A-66 lead directly to the vector equation Eq. A-67 for the toolface angle presented by Thorogood and Sawaryn[18]:

$$\tan\tau^* = \left(\frac{-\underline{b}^*\cdot\underline{r}^*}{-\underline{b}^*\cdot\underline{h}^*}\right). \quad \text{(A-67)}$$

The rightside unit vector lies in the horizontal plane, normal to both the $\underline{v}$ and $\underline{t}^*$ vectors, as shown in Eq. A-68. Evaluating the expression gives Eq. 7 in the body of the paper.

$$\underline{r}^* = \frac{\underline{v}\times\underline{t}^*}{\sin\theta^*}. \quad \text{(A-68)}$$

The highside unit vector lies in the vertical plane normal to both the $\underline{r}^*$ and $\underline{t}^*$ vectors, as shown in Eq. A-69. Combining Eq. A-68 with Eq. A-69, and expanding the triple vector product gives Eq. A-70. Evaluating the expression gives Eq. 6 in the body of the paper.

$$\underline{h}^* = \underline{r}^*\times\underline{t}^* \quad \text{(A-69)}$$

$$\underline{h}^* = \frac{\underline{t}^*\cos\theta^* - \underline{v}}{\sin\theta^*}. \quad \text{(A-70)}$$

The unit vector, $\underline{b}^*$, is normal to both the $\underline{t}^*$ and $\underline{n}_{12}$ vectors. Combining Eqs. A-8 and A-18 with Eq. A-71 gives Eq. A-72:

$$\underline{b}^* = \underline{t}^*\times\underline{n}_{12} \quad \text{(A-71)}$$

$$\underline{b}^* = \frac{\cos(\alpha-\alpha^*)\underline{t}_1 - \cos\alpha^*\,\underline{t}_2}{\sin\alpha}. \quad \text{(A-72)}$$

Taking the dot product of Eqs. A-72 and A-70 gives an expression for $(-\underline{b}^* \cdot \underline{h}^*)$, as shown in Eq. A-73. Taking the dot products gives Eq. A-74:

$$(-\underline{b}^* \cdot \underline{h}^*) = -\left[\frac{(\underline{t}^* \cdot \underline{t}_2)\underline{t}_1 - (\underline{t}^* \cdot \underline{t}_1)\underline{t}_2}{\sin\alpha}\right] \cdot \left(\frac{\underline{t}^* \cos\theta^* - \underline{v}}{\sin\theta^*}\right) \quad \text{(A-73)}$$

$$(-\underline{b}^* \cdot \underline{h}^*) = \frac{-\cos\alpha^* \cos\theta_2 + \cos(\alpha - \alpha^*)\cos\theta_1}{\sin\alpha \sin\theta^*}. \quad \text{(A-74)}$$

Taking the dot product of Eqs. A-72 and A-68 gives an expression for $(-\underline{b}^* \cdot \underline{r}^*)$, as shown in Eq. A-75:

$$(-\underline{b}^* \cdot \underline{r}^*) = \frac{\cos\alpha^*[\underline{t}_2 \cdot (\underline{v} \times \underline{t}^*)] - \cos(\alpha - \alpha^*)[\underline{t}_1 \cdot (\underline{v} \times \underline{t}^*)]}{\sin\alpha \sin\theta^*}. \quad \text{(A-75)}$$

By use of Eq. A-5, the scalar triple products in Eq. A-75 are given by Eqs. A-76 and A-77. Inserting these expressions into Eq. A-75 gives the final form for $(-\underline{b}^* \cdot \underline{r}^*)$, as shown in Eq. A-78:

$$\underline{t}_1 \cdot (\underline{v} \times \underline{t}^*) = -\sin\theta_1 \sin\theta^* \sin(\phi^* - \phi_1), \quad \text{(A-76)}$$

$$\underline{t}_2 \cdot (\underline{v} \times \underline{t}^*) = \sin\theta_2 \sin\theta^* \sin(\phi_2 - \phi^*), \quad \text{(A-77)}$$

$$(-\underline{b}^* \cdot \underline{r}^*) = \frac{\sin\theta_2 \cos\alpha^* \sin(\phi_2 - \phi^*) + \sin\theta_1 \cos(\alpha - \alpha^*)\sin(\phi^* - \phi_1)}{\sin\alpha}. \quad \text{(A–78)}$$

The general expression (Eq. 47) given in the body of the paper for toolface angle τ^*, is obtained by substituting Eqs. A-74 and A-78 into Eq. A-67.

Curvature. Referring to Fig. 16, Frenets[20] formula for total curvature, κ, gives Eq. A-79:

$$\frac{d\underline{t}^*}{dS^*} = -\kappa \underline{b}^*. \quad \text{(A-79)}$$

The definitions for κ_θ^* and κ_ϕ^* as the inclination and azimuthal components of the curvature, respectively, give Eqs. A-80 and A-81:

$$\frac{d\underline{t}^*}{dS^*} = \kappa_\theta^* \underline{h}^* \quad \text{(A-80)}$$

$$\text{and } \frac{1}{\sin\theta^*}\frac{d\underline{t}^*}{dS^*} = \kappa_\phi^* \underline{r}^*. \quad \text{(A-81)}$$

Eliminating the differential between Eqs. A-79 and A-80 and taking the dot product of both sides with $\underline{h}^*$ gives Eq. 51 for κ_θ^* in the body of the paper. The use of Eqs. A-65 and A-74 for $-\underline{b}^* \cdot \underline{h}^*$ gives Eq. 54 in the body of the paper.

Eliminating the differential between Eqs. A-79 and A-81, and taking the dot products of both sides with $\underline{r}^*$, gives Eq. 52 for κ_ϕ^* in the body of the paper. The use of Eqs. A-66 and A-78 for $-\underline{b}^* \cdot \underline{r}^*$ gives Eq. 55 in the body of the paper.

SI Metric Conversion Factors

ft × 3.048*	E–01	= m
° /100 ft × 0.984252	E–00	= ° /30 m

*Conversion factor is exact.

Steve Sawaryn is currently the Wells Team Leader, Engineering, for BP's Mature Business Unit in Aberdeen and is also the Drilling and Completions Adviser, specializing in drilling systems. During the last 26 years, he has held a variety of posts in drilling operations and consultancy, as well as in projects in Aberdeen, London, Kuwait, Alaska, and Norway. He is also a chartered engineer and fellow of the British Computer Soc. Sawaryn holds an MA degree in chemical engineering from Cambridge U. He is currently serving on the SPE Digital Energy Committee. **John Thorogood** is Chief Engineer for the BP Sakhalin exploration program, based in Yuzhno-Sakhalinsk, Russia. In addition, he is actively working on the issues associated with the operational command and control of drilling operations. He project managed the BP deepwater exploration operations in the Faroe Islands, U.K. sector, and in Norway from 1996 to 2001. He has 30 years of experience in drilling operations and technology, including his participation in the original deepwater wells west of Shetland in the early 1980s, and is the author of more than 40 papers on directional drilling, surveying, and deepwater operations. Thorogood holds BA and PhD degrees from Cambridge U. and is a member of the U.K. Inst. of Mechanical Engineers. He has served on the SPE Board of Directors with special responsibility for Drilling and Completions.